

A New Artificial Neural Network Space Vector PWM Controller for Voltage Source Inverter

Phan Quoc Dzung

Faculty of Electrical & Electronic Engineering
HCMC University of Technology
Ho Chi Minh City - Vietnam

Le Minh Phuong

Faculty of Electrical & Electronic Engineering
HCMC University of Technology
Ho Chi Minh City – Vietnam

Nguyen Van Nho

Faculty of Electrical & Electronic Engineering
HCMC University of Technology
Ho Chi Minh City - Vietnam

Abstract—This paper presents a new neural-network-based controller of space vector modulation (SVM) of a voltage-fed inverter. This ANN-SVPWM controller completely covers the undermodulation and overmodulation modes linearly extending operation smoothly up to square wave (six-step) by using theory of modulation between the limit trajectories with the famous linearity. The ANN controller has the advantage of very fast implementation of an SVM algorithm that can increase the switching frequency of power switches of the static converter. The design uses the individual training strategy with the fixed weight and supervised models. The ANN-SVPWM Controller can be used in V/Hz control technique and extended to a vector control method. A computer simulation program is developed using Matlab/Simulink together with the Neural Network Toolbox for training the ANN-controller.

Keyword: Space vector, Pulse-Width- Modulation, Artificial Neural Network, Voltage Source Inverter, undermodulation, overmodulation .

I. INTRODUCTION

Space Vector modulation (SVM) has recently grown as a very popular pulsewidth modulation (PWM) method for voltage – fed converter ac drives because of its very good harmonic quality and extended linear range of operation [1]. However, a difficulty of SVM is that it requires complex online computation that usually limits its operation up to several kilohertz of switching frequency. Switching frequency can be extended by using a high –speed DSP and simplifying computation with the help of lookup tables which is very large and tends to reduce the pulse width resolution.

Power switches recently have been improved in field of switching frequency. Modern ultrafast IGBTs allow operate at 50kHz. However, the DSP- based SVM practically fails in this region where artificial- neural – network (ANN) –based SVM can possibly take over [2].

The applications of ANN technique have been developed strongly in power electronic field in recent years. In the past, a neural network was implemented in instantaneous current control PWM [4-7]. Nevertheless, current control PWM does

not give optimum performance. Several researches of ANN implementation of SVM had been worked out [3,2]. Although this ANN-SVM controller has the advantage of fast calculation, the limitation of this approach is the difficulty of training in the overmodulation range with nonlinearity of modulation technique.

To avoid this spot, the proposed backpropagation-type feedforward ANN-SVM in this paper successfully have been trained by using two principal approaches:

- 1) Method of linear modulation between two limitary trajectories [8] (to overcome the difficulty of nonlinearity of overmodulation range)
- 2) Individual training strategy with 8 Sub-nets (to overcome the complexity of SVM for 3 mode : undermodulation, overmodulation mode 1, overmodulation mode 2).

II. SPACE- VECTOR PWM IN UNDERMODULATION AND OVERMODULATION REGIONS

The SVM technique has been well discussed and developed in literature, and a number of authors [1], [8]-[10] have described its operation in the overmodulation. Among these methods of modulation, method of modulation between trajectories [8] has the advantage of simplicity and linearity.

A. Undermodulation ($0 < M < 0.907$)

In the undermodulation, the rotating reference voltage remains within the hexagon. The SVM strategy in this region is based on generating three consecutive switching voltage vectors in a sampling period (T_s) such that the average output voltage matches with the reference voltage. The equations for effective duty cycle of the inverter switching states can be described as following :

$$\begin{aligned}d_1 &= \sqrt{3}M \sin(\pi/3 - \alpha) \\d_2 &= \sqrt{3}M \sin(\alpha) \\d_0 &= 1 - d_1 - d_2\end{aligned}\tag{1}$$

where

d_1 - duty cycle ($2t_1/T_s$) of switching vector that lags
 d_2 - duty cycle ($2t_2/T_s$) of switching vector that leads
 d_0 - duty cycle ($2t_0/T_s$) of zero-switching vector
 M - modulation factor $M = V^*/V_{1sw}$ (V^* - magnitude of reference voltage vector, V_{1sw} – the peak value of six-step voltage wave).

The timing intervals are obtained by multiplying duty cycles and periode $T_s/2$ respectively.

B. Overmodulation mode 1 ($0.907 < M < 0.952$)

This mode starts when the reference voltage V^* exceeds the inscribable circle in the hexagon and attains the sides of the hexagon. On the hexagon trajectory, duty d_0 vanish :

$$\begin{aligned} d_1^* &= \frac{\sqrt{3} \cos \alpha - \sin \alpha}{\sqrt{3} \cos \alpha + \sin \alpha} \\ d_2^* &= 1 - d_1 \\ d_0^* &= 0 \end{aligned} \quad (2)$$

Applying theory of linear modulation within trajectory, the first trajectory has been chosen with $M = 0.907$:

$$\begin{aligned} d_1^* &= \sqrt{3} \cdot 0.907 \sin(\pi/3 - \alpha) \\ d_2^* &= \sqrt{3} \cdot 0.907 \sin(\alpha) \\ d_0^* &= 1 - d_1 - d_2 \end{aligned} \quad (3)$$

The second one is the boundary of hexagon (2).

Coefficient of modulation is defined as following :

$$\eta = \frac{M - M_1}{M_2 - M_1} \quad (4)$$

The duty cycles accordingly [8] are determined as :

$$\begin{aligned} d_1 &= d_1^* + \eta(d_1^{**} - d_1^*) \\ d_2 &= d_2^* + \eta(d_2^{**} - d_2^*) \\ d_0 &= d_0^* + \eta(-d_0^*) \end{aligned} \quad (5)$$

C. Overmodulation mode 2 ($0.952 < M < 1$)

In overmodulation mode 2, the reference vector V^* increases further up to six-step mode.

Applying theory of linear modulation within trajectory, the first trajectory has been chosen with $M = 0.952$:

$$\begin{aligned} d_1^* &= \frac{\sqrt{3} \cos \alpha - \sin \alpha}{\sqrt{3} \cos \alpha + \sin \alpha} \\ d_2^* &= 1 - d_1 \\ d_0^* &= 0 \end{aligned} \quad (6)$$

The second is divided in two cases :

- For $0 < \alpha < \pi/6$:

$$d_1^* = 1; d_2^* = 0; d_0^* = 0 \quad (7)$$

- For $\pi/6 < \alpha < \pi/3$:

$$d_1^* = 0; d_2^* = 1; d_0^* = 0 \quad (8)$$

Accordingly [8], the duty cycles are described linearly as following:

$$\begin{aligned} d_1 &= d_1^* + \eta(d_1^{**} - d_1^*) \\ d_2 &= d_2^* + \eta(d_2^{**} - d_2^*) \\ d_0 &= 0 \end{aligned} \quad (9)$$

Coefficient η is determined similarly (4) where $M_1=0.952$, $M_2=1$.

In overmodulation region, this approach has the advantage of simplicity in comparison with other conventional method [2].

III. NEURAL-NETWORK-BASED SPACE- VECTOR PWM CONTROLLER

The SVM algorithm described in the previous section will be used to obtain training data for proposed ANN-SVM.

A. Undermodulation Region Sub-net :

For any command angle α^* , the duty cycles d_1 , d_2 , d_0 are given by (1) for sector $\theta = 1$. Similar duty cycles can be determined for all six sectors and the phase turn-on duty cycles can be calculated as :

1) For sector 1: ($0 < \alpha^* < \pi/3$)

$$d_{A-ON} = \frac{d_0}{2} = \frac{1}{2} + \frac{\sqrt{3}}{2} \cdot M \cdot (-\sin(\pi/3 - \alpha) - \sin \alpha) \quad (10)$$

$$d_{B-ON} = \frac{d_0}{2} + d_1 = \frac{1}{2} + \frac{\sqrt{3}}{2} \cdot M \cdot (\sin(\pi/3 - \alpha) - \sin \alpha)$$

$$d_{C-ON} = \frac{d_0}{2} + d_1 + d_2 = \frac{1}{2} + \frac{\sqrt{3}}{2} \cdot M \cdot (\sin(\pi/3 - \alpha) + \sin \alpha)$$

2) For sector 2: ($\pi/3 < \alpha^* < 2\pi/3$)

$$d_{A-ON} = \frac{d_0}{2} + d_2 = \frac{1}{2} + \frac{\sqrt{3}}{2} \cdot M \cdot (-\sin(\pi/3 - \alpha) + \sin \alpha) \quad (11)$$

$$d_{B-ON} = \frac{d_0}{2} = \frac{1}{2} + \frac{\sqrt{3}}{2} \cdot M \cdot (-\sin(\pi/3 - \alpha) - \sin \alpha)$$

$$d_{C-ON} = \frac{d_0}{2} + d_1 + d_2 = \frac{1}{2} + \frac{\sqrt{3}}{2} \cdot M \cdot (\sin(\pi/3 - \alpha) + \sin \alpha)$$

3) For sector 3: ($2\pi/3 < \alpha^* < \pi$)

$$d_{A-ON} = \frac{d_0}{2} + d_1 + d_2 = \frac{1}{2} + \frac{\sqrt{3}}{2} \cdot M \cdot (\sin(\pi/3 - \alpha) + \sin \alpha) \quad (12)$$

$$d_{B-ON} = \frac{d_0}{2} = \frac{1}{2} + \frac{\sqrt{3}}{2} \cdot M \cdot (-\sin(\pi/3 - \alpha) - \sin \alpha)$$

$$d_{C-ON} = \frac{d_0}{2} + d_1 = \frac{1}{2} + \frac{\sqrt{3}}{2} \cdot M \cdot (\sin(\pi/3 - \alpha) - \sin \alpha)$$

4) For sector 4: ($\pi < \alpha^* < 4\pi/3$)

$$d_{A-ON} = \frac{d_0}{2} + d_1 + d_2 = \frac{1}{2} + \frac{\sqrt{3}}{2} \cdot M \cdot (\sin(\pi/3 - \alpha) + \sin \alpha) \quad (13)$$

$$d_{B-ON} = \frac{d_0}{2} + d_2 = \frac{1}{2} + \frac{\sqrt{3}}{2} \cdot M \cdot (-\sin(\pi/3 - \alpha) + \sin \alpha)$$

$$d_{C-ON} = \frac{d_0}{2} = \frac{1}{2} + \frac{\sqrt{3}}{2} \cdot M \cdot (-\sin(\pi/3 - \alpha) - \sin \alpha)$$

5) For sector 5: ($4\pi/3 < \alpha^* < 5\pi/3$)

$$d_{A-ON} = \frac{d_0}{2} + d_1 = \frac{1}{2} + \frac{\sqrt{3}}{2} \cdot M \cdot (\sin(\pi/3 - \alpha) - \sin \alpha) \quad (14)$$

$$d_{B-ON} = \frac{d_0}{2} + d_1 + d_2 = \frac{1}{2} + \frac{\sqrt{3}}{2} \cdot M \cdot (\sin(\pi/3 - \alpha) + \sin \alpha)$$

$$d_{C-ON} = \frac{d_0}{2} = \frac{1}{2} + \frac{\sqrt{3}}{2} \cdot M \cdot (-\sin(\pi/3 - \alpha) - \sin \alpha)$$

6) For sector 6: ($5\pi/3 < \alpha^* < 2\pi$)

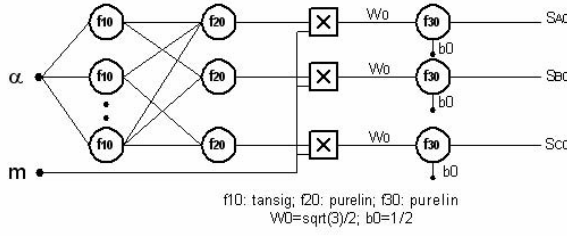


Figure 1. Undermodulation region subnet

$$d_{A-ON} = \frac{d_0}{2} = \frac{1}{2} + \frac{\sqrt{3}}{2} \cdot M \cdot (-\sin(\pi/3 - \alpha) - \sin \alpha) \quad (15)$$

$$d_{B-ON} = \frac{d_0}{2} + d_1 + d_2 = \frac{1}{2} + \frac{\sqrt{3}}{2} \cdot M \cdot (\sin(\pi/3 - \alpha) + \sin \alpha)$$

$$d_{C-ON} = \frac{d_0}{2} + d_2 = \frac{1}{2} + \frac{\sqrt{3}}{2} \cdot M \cdot (-\sin(\pi/3 - \alpha) + \sin \alpha)$$

Hence, the turn-on and turn-off time interval are determined as following :

$$T_{A,B,C-ON} = d_{A,B,C-ON} \cdot \frac{T_s}{2} \quad (16)$$

$$T_{A,B,C-OFF} = (1 - d_{A,B,C-ON}) \cdot \frac{T_s}{2}$$

Equation (10)-(15) can transform in general form :

$$d_{A-ON} = \frac{1}{2} + M \cdot h_{10}(\alpha^*) \quad (17)$$

$$d_{B-ON} = \frac{1}{2} + M \cdot h_{20}(\alpha^*)$$

$$d_{C-ON} = \frac{1}{2} + M \cdot h_{30}(\alpha^*)$$

where

$$h_{10}(\alpha^*) = \begin{cases} \frac{\sqrt{3}}{2} [-\sin(\pi/3 - \alpha) - \sin \alpha] & \theta = 1, 6 \\ \frac{\sqrt{3}}{2} [-\sin(\pi/3 - \alpha) + \sin \alpha] & \theta = 2 \\ \frac{\sqrt{3}}{2} [+ \sin(\pi/3 - \alpha) + \sin \alpha] & \theta = 3, 4 \\ \frac{\sqrt{3}}{2} [+ \sin(\pi/3 - \alpha) - \sin \alpha] & \theta = 5 \end{cases} \quad (16)$$

$h_{20}(\alpha^*)$, $h_{30}(\alpha^*)$ are obtained similarly. Then, $h_{10,20,30}(\alpha^*)$ have been used for creating databases which are needed for training undermodulation region Sub-net with one input (α^*) and three outputs (h_{10} , h_{20} , h_{30}). The angle step is 1 degree.

A two-layer network is used for implementing this Sub-net. The sub-net is obtained by training (supervised) with *trainlm* function – Levenberg –Marquardt algorithm, the acceptable for training squared error is 10^{-4} . The number of neurons of 1st layer is 10 *tansig* neurons, the 2nd layer has 3 *purelin* neurons. So, the total number of neurons is 13 neurons (convergence obtained for 354 epochs).

For implementing undermodulation duty cycles (equations (17)), it can be used one further product net-input-function (inputs : $h(\alpha^*)$, M) and one *purelin* neuron (weight = 1, bias = 0.5) (Fig.1)

B. Overmodulation mode1 Sub-net :

The duty cycles d_1 , d_2 , d_0 are calculated by (5) for sector $\theta = 1$. After several substitutions, the duty cycles can be described as :

$$d_1 = K_2 \sin(\pi/3 - \alpha) + \eta \left[-K_2 \sin(\pi/3 - \alpha) + \frac{K_1 \cos \alpha - \sin \alpha}{K_1 \cos \alpha + \sin \alpha} \right] \quad (17)$$

$$d_2 = 1 - \frac{K_1 \cos \alpha - \sin \alpha}{K_1 \cos \alpha + \sin \alpha} + \eta \left[-K_2 \sin \alpha + 1 - \frac{K_1 \cos \alpha - \sin \alpha}{K_1 \cos \alpha + \sin \alpha} \right]$$

$$d_0 = 1 - d_1 - d_2$$

where

$$K_1 = \sqrt{3}; \quad K_2 = \sqrt{3} \cdot 0.907$$

Duty cycles can be determined for all six sectors and the phase turn-on duty cycles can be calculated similar as (10)-(15) by substituting (17).

1) For sector 1: ($0 < \alpha^* < \pi/3$)

$$d_{A-ON} = \frac{d_0}{2} = \frac{1}{2} + \frac{1}{2} \cdot \left[\left(-K_2 \sin(\pi/3 - \alpha) - 1 + \frac{K_1 \cos \alpha - \sin \alpha}{K_1 \cos \alpha + \sin \alpha} \right) + \eta(-1 + K_2(\sin(\pi/3 - \alpha) + \sin \alpha)) \right]$$

$$d_{B-ON} = \frac{d_0}{2} + d_1 = \frac{1}{2} + \frac{1}{2} \cdot \left[\left(K_2 \sin(\pi/3 - \alpha) - 1 + \frac{K_1 \cos \alpha - \sin \alpha}{K_1 \cos \alpha + \sin \alpha} \right) + \eta \left(-1 + K_2(\sin(\pi/3 - \alpha) + \sin \alpha) + 2 \cdot \frac{K_1 \cos \alpha - \sin \alpha}{K_1 \cos \alpha + \sin \alpha} \right) \right]$$

$$d_{C-ON} = \frac{d_0}{2} + d_1 + d_2 = \frac{1}{2} + \frac{1}{2} \cdot \left[\left(K_2 \sin(\pi/3 - \alpha) + 1 - \frac{K_1 \cos \alpha - \sin \alpha}{K_1 \cos \alpha + \sin \alpha} \right) + \eta(1 - K_2(\sin(\pi/3 - \alpha) + \sin \alpha)) \right] \quad (18)$$

2) For sector 2: ($\pi/3 < \alpha^* < 2\pi/3$)

$$d_{A-ON} = \frac{d_0}{2} + d_2 = \frac{1}{2} + \frac{1}{2} \cdot \left[\left(-K_2 \sin(\pi/3 - \alpha) + 1 - \frac{K_1 \cos \alpha - \sin \alpha}{K_1 \cos \alpha + \sin \alpha} \right) + \eta \left(K_2(\sin(\pi/3 - \alpha) + \sin \alpha) + 1 - 2 \cdot \frac{K_1 \cos \alpha - \sin \alpha}{K_1 \cos \alpha + \sin \alpha} \right) \right]$$

$$d_{B-ON} = \frac{d_0}{2} = \frac{1}{2} + \frac{1}{2} \cdot \left[\left(-K_2 \sin(\pi/3 - \alpha) - 1 + \frac{K_1 \cos \alpha - \sin \alpha}{K_1 \cos \alpha + \sin \alpha} \right) + \eta(-1 + K_2(\sin(\pi/3 - \alpha) + \sin \alpha)) \right]$$

$$d_{C-ON} = \frac{d_0}{2} + d_1 + d_2 = \frac{1}{2} + \frac{1}{2} \cdot \left[\left(K_2 \sin(\pi/3 - \alpha) + 1 - \frac{K_1 \cos \alpha - \sin \alpha}{K_1 \cos \alpha + \sin \alpha} \right) + \eta(1 - K_2(\sin(\pi/3 - \alpha) + \sin \alpha)) \right] \quad (19)$$

3) For sector 3: ($2\pi/3 < \alpha^* < \pi$)

$$d_{A-ON} = \frac{d_0}{2} + d_1 + d_2 = \frac{1}{2} + \frac{1}{2} \cdot \left[\left(K_2 \sin(\pi/3 - \alpha) + 1 - \frac{K_1 \cos \alpha - \sin \alpha}{K_1 \cos \alpha + \sin \alpha} \right) + \eta(1 - K_2(\sin(\pi/3 - \alpha) + \sin \alpha)) \right]$$

$$d_{B-ON} = \frac{d_0}{2} = \frac{1}{2} + \frac{1}{2} \cdot \left[\left(-K_2 \sin(\pi/3 - \alpha) - 1 + \frac{K_1 \cos \alpha - \sin \alpha}{K_1 \cos \alpha + \sin \alpha} \right) + \eta(-1 + K_2(\sin(\pi/3 - \alpha) + \sin \alpha)) \right]$$

$$d_{C-ON} = \frac{d_0}{2} + d_1 = \frac{1}{2} + \frac{1}{2} \cdot \left[\left(K_2 \sin(\pi/3 - \alpha) - 1 + \frac{K_1 \cos \alpha - \sin \alpha}{K_1 \cos \alpha + \sin \alpha} \right) + \eta \left(-1 + K_2(\sin(\pi/3 - \alpha) + \sin \alpha) + 2 \cdot \frac{K_1 \cos \alpha - \sin \alpha}{K_1 \cos \alpha + \sin \alpha} \right) \right] \quad (20)$$

4) For sector 4: ($\pi < \alpha^* < 4\pi/3$)

$$\begin{aligned} d_{A-OV} &= \frac{d_0}{2} + d_1 + d_2 = \frac{1}{2} + \frac{1}{2} \cdot \left[\left(K_2 \sin(\pi/3 - \alpha) + 1 - \frac{K_1 \cos \alpha - \sin \alpha}{K_1 \cos \alpha + \sin \alpha} \right) + \right. \\ &\quad \left. \eta(1 - K_2(\sin(\pi/3 - \alpha) + \sin \alpha)) \right] \\ d_{B-OV} &= \frac{d_0}{2} + d_2 = \frac{1}{2} + \frac{1}{2} \cdot \left[\left(-K_2 \sin(\pi/3 - \alpha) + 1 - \frac{K_1 \cos \alpha - \sin \alpha}{K_1 \cos \alpha + \sin \alpha} \right) + \right. \\ &\quad \left. \eta \left(K_2(\sin(\pi/3 - \alpha) + \sin \alpha) + 1 - 2 \cdot \frac{K_1 \cos \alpha - \sin \alpha}{K_1 \cos \alpha + \sin \alpha} \right) \right] \\ d_{C-OV} &= \frac{d_0}{2} = \frac{1}{2} + \frac{1}{2} \cdot \left[\left(-K_2 \sin(\pi/3 - \alpha) - 1 + \frac{K_1 \cos \alpha - \sin \alpha}{K_1 \cos \alpha + \sin \alpha} \right) + \right. \\ &\quad \left. \eta(-1 + K_2(\sin(\pi/3 - \alpha) + \sin \alpha)) \right] \end{aligned} \quad (21)$$

5) For sector 5: ($4\pi/3 < \alpha^* < 5\pi/3$)

$$\begin{aligned} d_{A-OV} &= \frac{d_0}{2} + d_1 = \frac{1}{2} + \frac{1}{2} \cdot \left[\left(K_2 \sin(\pi/3 - \alpha) - 1 + \frac{K_1 \cos \alpha - \sin \alpha}{K_1 \cos \alpha + \sin \alpha} \right) + \right. \\ &\quad \left. \eta \left(-1 + K_2(\sin(\pi/3 - \alpha) + \sin \alpha) + 2 \cdot \frac{K_1 \cos \alpha - \sin \alpha}{K_1 \cos \alpha + \sin \alpha} \right) \right] \\ d_{B-OV} &= \frac{d_0}{2} + d_1 + d_2 = \frac{1}{2} + \frac{1}{2} \cdot \left[\left(K_2 \sin(\pi/3 - \alpha) + 1 - \frac{K_1 \cos \alpha - \sin \alpha}{K_1 \cos \alpha + \sin \alpha} \right) + \right. \\ &\quad \left. \eta(1 - K_2(\sin(\pi/3 - \alpha) + \sin \alpha)) \right] \\ d_{C-OV} &= \frac{d_0}{2} = \frac{1}{2} + \frac{1}{2} \cdot \left[\left(-K_2 \sin(\pi/3 - \alpha) - 1 + \frac{K_1 \cos \alpha - \sin \alpha}{K_1 \cos \alpha + \sin \alpha} \right) + \right. \\ &\quad \left. \eta(-1 + K_2(\sin(\pi/3 - \alpha) + \sin \alpha)) \right] \end{aligned} \quad (22)$$

6) For sector 6: ($5\pi/3 < \alpha^* < 2\pi$)

$$\begin{aligned} d_{A-OV} &= \frac{d_0}{2} = \frac{1}{2} + \frac{1}{2} \cdot \left[\left(-K_2 \sin(\pi/3 - \alpha) - 1 + \frac{K_1 \cos \alpha - \sin \alpha}{K_1 \cos \alpha + \sin \alpha} \right) + \right. \\ &\quad \left. \eta(-1 + K_2(\sin(\pi/3 - \alpha) + \sin \alpha)) \right] \\ d_{B-OV} &= \frac{d_0}{2} + d_1 + d_2 = \frac{1}{2} + \frac{1}{2} \cdot \left[\left(K_2 \sin(\pi/3 - \alpha) + 1 - \frac{K_1 \cos \alpha - \sin \alpha}{K_1 \cos \alpha + \sin \alpha} \right) + \right. \\ &\quad \left. \eta(1 - K_2(\sin(\pi/3 - \alpha) + \sin \alpha)) \right] \\ d_{C-OV} &= \frac{d_0}{2} + d_2 = \frac{1}{2} + \frac{1}{2} \cdot \left[\left(-K_2 \sin(\pi/3 - \alpha) + 1 - \frac{K_1 \cos \alpha - \sin \alpha}{K_1 \cos \alpha + \sin \alpha} \right) + \right. \\ &\quad \left. \eta \left(K_2(\sin(\pi/3 - \alpha) + \sin \alpha) + 1 - 2 \cdot \frac{K_1 \cos \alpha - \sin \alpha}{K_1 \cos \alpha + \sin \alpha} \right) \right] \end{aligned} \quad (23)$$

Equations (18)-(23) can be transform in general forme :

$$d_{A-OV} = \frac{1}{2} + \frac{1}{2} [h_{11a}(\alpha^*) + \eta \cdot h_{21a}(\alpha^*)] \quad (24)$$

$$d_{B-OV} = \frac{1}{2} + \frac{1}{2} [h_{11b}(\alpha^*) + \eta \cdot h_{21b}(\alpha^*)]$$

$$d_{C-OV} = \frac{1}{2} + \frac{1}{2} [h_{11c}(\alpha^*) + \eta \cdot h_{21c}(\alpha^*)]$$

where

$$h_{11a}(\alpha^*) = \begin{cases} -K_2 \sin(\pi/3 - \alpha) - 1 + \frac{K_1 \cos \alpha - \sin \alpha}{K_1 \cos \alpha + \sin \alpha}, & \theta = 1, 6 \\ -K_2 \sin(\pi/3 - \alpha) - 1 - \frac{K_1 \cos \alpha - \sin \alpha}{K_1 \cos \alpha + \sin \alpha}, & \theta = 2 \\ +K_2 \sin(\pi/3 - \alpha) - 1 - \frac{K_1 \cos \alpha - \sin \alpha}{K_1 \cos \alpha + \sin \alpha}, & \theta = 3, 4 \\ K_2 \sin(\pi/3 - \alpha) - 1 + \frac{K_1 \cos \alpha - \sin \alpha}{K_1 \cos \alpha + \sin \alpha}, & \theta = 5 \end{cases} \quad (25)$$

and

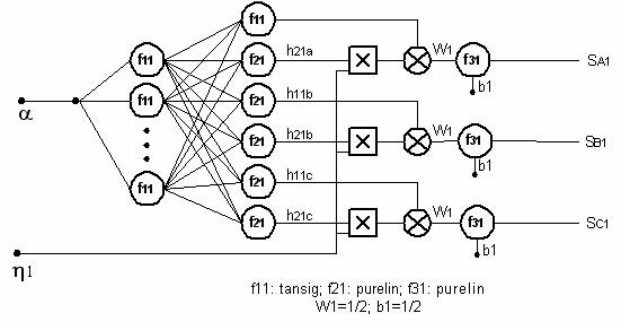


Figure 2. Overmodulation mode 1 region subnet

$$h_{21a}(\alpha^*) = \begin{cases} -1 + K_2(\sin(\pi/3 - \alpha) + \sin \alpha), & \theta = 1, 6 \\ K_2(\sin(\pi/3 - \alpha) + \sin \alpha) + 1 - 2 \cdot \frac{K_1 \cos \alpha - \sin \alpha}{K_1 \cos \alpha + \sin \alpha}, & \theta = 2 \\ 1 - K_2(\sin(\pi/3 - \alpha) + \sin \alpha), & \theta = 3, 4 \\ -1 + K_2(\sin(\pi/3 - \alpha) + \sin \alpha) + 2 \cdot \frac{K_1 \cos \alpha - \sin \alpha}{K_1 \cos \alpha + \sin \alpha}, & \theta = 5 \end{cases} \quad (26)$$

$h_{11b}(\alpha^*)$, $h_{21b}(\alpha^*)$, $h_{11c}(\alpha^*)$, $h_{21c}(\alpha^*)$ are obtained similarly. Then, h_{11a} , h_{21a} , h_{11b} , h_{21b} , h_{11c} , $h_{21c}(\alpha^*)$ have been used for creating databases which are needed for training overmodulation region Sub-net with one input (α^*) and six outputs (h_{11a} , h_{21a} , h_{11b} , h_{21b} , h_{11c} , h_{21c}). The angle step is 1 degree.

A two-layer network is used for implementing this Sub-net. The sub-net is obtained by training (supervised) with *trainlm* function – Levenberg –Marquardt algorithm, the acceptable for training squared error is 10^{-4} . The number of neurons of 1st layer is 20 *tansig* neurons, the 2nd layer has 6 *purelin* neurons. So, the total number of neurons is 26 neurons (convergence obtained for 4365 epochs).

For implementing complete overmodulation duty cycles in equations (24), it can be used one further product net-input-function (inputs : $h_{21}(\alpha^*)$, η), one further sum net-input-function (inputs : $h_{11}(\alpha^*)$, $\eta * h_{21}(\alpha^*)$) and one purelin neuron (weight = 0.5, bias = 0.5) (Fig.2).

C. Overmodulation mode 2 Sub-net :

The duty cycles in this mode d_1 , d_2 , d_0 are given by (9) for sector $\theta = 1$. After several transformations, the duty cycles can be written as :

- For $0 < \alpha \leq \pi/6$:

$$d_1 = \frac{\sqrt{3} \cos \alpha - \sin \alpha}{\sqrt{3} \cos \alpha + \sin \alpha} + \eta \left(1 - \frac{\sqrt{3} \cos \alpha - \sin \alpha}{\sqrt{3} \cos \alpha + \sin \alpha} \right) \quad (27)$$

$$d_2 = 1 - \frac{\sqrt{3} \cos \alpha - \sin \alpha}{\sqrt{3} \cos \alpha + \sin \alpha} + \eta \left[\frac{\sqrt{3} \cos \alpha - \sin \alpha}{\sqrt{3} \cos \alpha + \sin \alpha} - 1 \right]$$

$$d_0 = 0$$

- For $\pi/6 < \alpha \leq \pi/3$:

$$d_1 = \frac{\sqrt{3} \cos \alpha - \sin \alpha}{\sqrt{3} \cos \alpha + \sin \alpha} + \eta \cdot \frac{\sqrt{3} \cos \alpha - \sin \alpha}{\sqrt{3} \cos \alpha + \sin \alpha} \quad (28)$$

$$d_2 = 1 - \frac{\sqrt{3} \cos \alpha - \sin \alpha}{\sqrt{3} \cos \alpha + \sin \alpha} + \eta \cdot \frac{\sqrt{3} \cos \alpha - \sin \alpha}{\sqrt{3} \cos \alpha + \sin \alpha}$$

$$d_0 = 0$$

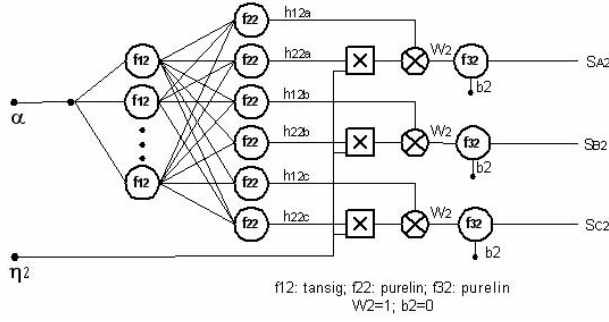


Figure 3. Overmodulation mode 2 region subnet

Duty cycles can be expressed for all six sectors by using (28):

$$1) \text{ For sector 1: } (0 < \alpha^* < \pi/3) \quad (29)$$

$$d_{A-ON} = 0; d_{B-ON} = d_1; d_{C-ON} = \frac{1}{2}$$

$$2) \text{ For sector 2: } (\pi/3 < \alpha^* < 2\pi/3) \quad (30)$$

$$d_{A-ON} = d_2; d_{B-ON} = 0; d_{C-ON} = \frac{1}{2}$$

$$3) \text{ For sector 3: } (2\pi/3 < \alpha^* < \pi) \quad (31)$$

$$d_{A-ON} = \frac{1}{2}; d_{B-ON} = 0; d_{C-ON} = d_1$$

$$4) \text{ For sector 4: } (\pi < \alpha^* < 4\pi/3) \quad (32)$$

$$d_{A-ON} = \frac{1}{2}; d_{B-ON} = d_2; d_{C-ON} = 0$$

$$5) \text{ For sector 5: } (4\pi/3 < \alpha^* < 5\pi/3) \quad (33)$$

$$d_{A-ON} = d_1; d_{B-ON} = \frac{1}{2}; d_{C-ON} = 0$$

$$6) \text{ For sector 6: } (5\pi/3 < \alpha^* < 2\pi) \quad (34)$$

$$d_{A-ON} = 0; d_{B-ON} = \frac{1}{2}; d_{C-ON} = d_2$$

Equations (29)-(34) can be written in general form :

$$d_{A-ON} = h_{12a}(\alpha^*) + \eta \cdot h_{22a}(\alpha^*) \quad (35)$$

$$d_{B-ON} = h_{12b}(\alpha^*) + \eta \cdot h_{22b}(\alpha^*)$$

$$d_{C-ON} = h_{12c}(\alpha^*) + \eta \cdot h_{22c}(\alpha^*)$$

where

$$h_{21a}(\alpha^*) = \begin{cases} 0, & \theta = 1, 6 \\ 1 - \frac{\sqrt{3} \cos \alpha - \sin \alpha}{\sqrt{3} \cos \alpha + \sin \alpha}, & \theta = 2 \\ 0.5, & \theta = 3, 4 \\ \frac{\sqrt{3} \cos \alpha - \sin \alpha}{\sqrt{3} \cos \alpha + \sin \alpha}, & \theta = 5 \end{cases} \quad (36)$$

and

$$h_{21a}(\alpha^*) = \begin{cases} 0, & \theta = 1, 6 \\ 1 - \frac{\sqrt{3} \cos \alpha - \sin \alpha}{\sqrt{3} \cos \alpha + \sin \alpha}, & \text{for } 0 \leq \alpha \leq \pi/6 \\ \frac{\sqrt{3} \cos \alpha - \sin \alpha}{\sqrt{3} \cos \alpha + \sin \alpha}, & \text{for } \pi/6 \leq \alpha \leq \pi/3 \\ 0, & \theta = 3, 4 \\ 1 - \frac{\sqrt{3} \cos \alpha - \sin \alpha}{\sqrt{3} \cos \alpha + \sin \alpha}, & \text{for } 0 \leq \alpha \leq \pi/6 \\ \frac{\sqrt{3} \cos \alpha - \sin \alpha}{\sqrt{3} \cos \alpha + \sin \alpha}, & \text{for } \pi/6 \leq \alpha \leq \pi/3 \end{cases} \quad (37)$$

$h_{21b}(\alpha^*), h_{22b}(\alpha^*), h_{21c}(\alpha^*), h_{22c}(\alpha^*)$ are obtained similarly. Then, $h_{21a, 22a, 21b, 22b, 21c, 22c}(\alpha^*)$ have been used for creating databases which are needed for training overmodulation mode 2 Sub-net with one input (α^*) and six outputs ($h_{21a}, h_{22a}, h_{21b}, h_{22b}, h_{21c}, h_{22c}$). The angle step is 1 degree.

A two-layer network is used for implementing this Sub-net. The sub-net is obtained by training (supervised) with *trainlm* function – Levenberg –Marquardt algorithm, the acceptable for training squared error is 10^{-4} . The number of neurons of 1st layer is 20 *tansig* neurons, the 2nd layer has 6 *purelin* neurons. So, the total number of neurons is 26 neurons (convergence obtained for 1433 epochs).

For implementing complete overmodulation duty cycles in equations (35), it can be designed one further product net-input-function (inputs : $h_{22}(\alpha^*), \eta$), one further sum net-input-function (inputs : $h_{21}(\alpha^*), \eta h_{22}(\alpha^*)$) and one purelin neuron (weight = 1, bias = 0) (Fig.3).

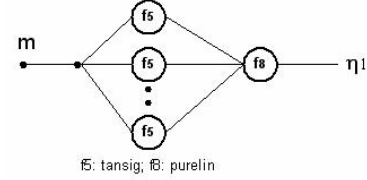


Figure 4. η_1 calculation subnet

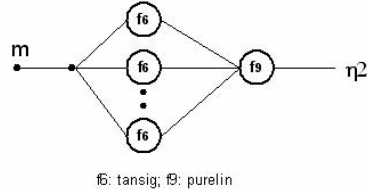


Figure 5. η_2 calculation subnet

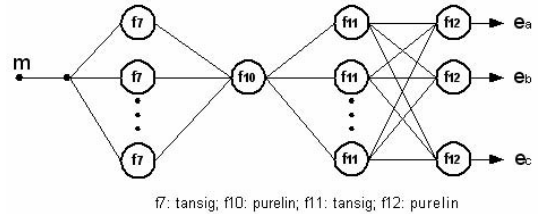


Figure 6. Code of modulation mode Sub-net

D. η_1, η_2 calculation Sub-nets :

The coefficient η_1 and η_2 in overmodulation mode 1 and mode 2 respectively are given by equation (4). This equation had been used for generating neural network training data. The input M is varied from 0.907 to 0.952 with step of 0.001, the output is η_1 and varied from 0.952 to 1 with step of 0.001, the output is η_2 .

A 2-layer network is used for implementing these sub-nets. The sub-net is obtained by training (supervised) with *trainlm* function – Levenberg –Marquardt algorithm, the acceptable for training squared error is 10^{-4} . The number of neurons of 1st layer is 1 *tansig* neurons, the 2nd layer has 1 *purelin* neurons. So, the total number of neurons is 2 neurons. Convergence is obtained for 57 epochs for η_1 -subnet and 46 epochs for η_2 -subnet) (Fig. 4, 5).

E. Code of modulation mode Sub-net :

The purpose of this subnet is to define the code of modulation mode :

- undermodulation : $C_m = 0$
- overmodulation mode 1 : $C_m = 1$
- overmodulation mode 2 : $C_m = 2$

The input M is varied from 0 to 1 with step of 0.001, the output is C_m .

The sub-net is trained with *trainlm* function – Levenberg – Marquardt algorithm, the acceptable for training squared error is 10^{-4} . The number of neurons of 1st layer is 4 *tansig* neurons, the 2nd layer has 1 *purelin* neurons. So, the total number of neurons is 5 neurons. Convergence is obtained for 118 epochs.

F. Mode Selection Code Sub-net :

This subnet is used for determining which modulation mode to be choice for generating duty cycles at outputs of ANN-SVM-Controller (S_A, S_B, S_C).

The input of this subnet is C_m , the output is e_A, e_B, e_C (Table 1). (Fig.6)

TABLE I. MODE SELECTION CODE

C_m	e_A	e_B	e_C
0	1	0	0
1	0	1	0
2	0	0	1

The sub-net is trained with *trainlm* function – Levenberg – Marquardt algorithm, the acceptable for training squared error is 10^{-10} . The number of neurons of 1st layer is 2 *logsig* neurons, the 2nd layer has 3 *purelin* neurons. So, the total number of neurons is 5 neurons. Convergence is obtained for a few (4) epochs.

A complete proposed ANN-SVM Controller is presented in Fig.1. This ANN-Controller consists of 8 layers and about one hundred neurons. The ANN-Controller has 2 inputs (α, M) and 3 outputs ($WT_{A-ON}, WT_{B-ON}, WT_{C-ON}$). The outputs are the digital words corresponding to turn-on times which are

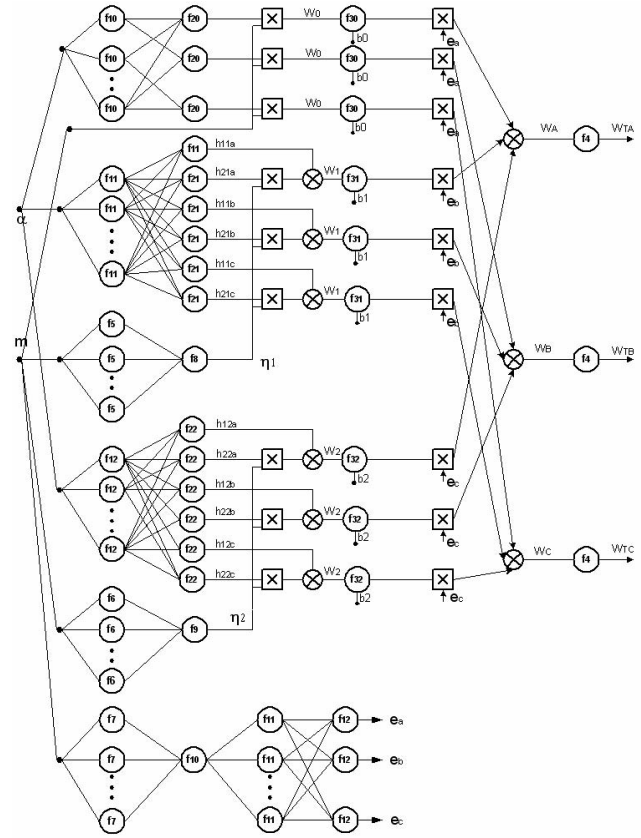


Figure 7. Complete ANN-SVM-Controller for VSI

generated by multiplying the duty cycles S_A, S_B, S_C by the value of sample time T_s .

III. SIMULATION OF ANN-SVM-CONTROLLER

A Simulink/Matlab program with the toolbox of neural – network is used to train and simulate the complete ANN-SVM Controller with the above-mentioned sub-nets for different mode of operation : undermodulation, overmodulation.

Simulation results demonstrate the excellent performance of the proposed ANN_SVM Controller with acceptable error of duty cycles about 10^{-4} as demonstrated before (training squared error).

IV. CONCLUSION

This paper presents a new complete artificial-neural-network space- vector- modulation controller (ANN-SVM-Controller) scheme for a Voltage Source Inverter that operates very well in undermodulation as well as in overmodulation (Mode –1 and Mode-2) regions. The digital words corresponding to turn-on time are generated by the ANN and then converted to pulse widths through a timer. Two principal approaches have been used successfully : *Method of linear modulation between two limitary trajectories extended to six-step mode* and *Individual training strategy*. The training data and training time are reasonably small. The training procedure are easy and reliable.

In the practical field, the proposed ANN-SVM-Controller can be implemented with V/Hz-controlled and vector controlled induction motor drives. The ANN based SVM can give higher switching frequency, which is not possible by conventional DSP- based SVM [2]. ANN-SVM-Controller may be implemented by ASIC chip in the future.

REFERENCE

- [1] J. Holtz "Pulse width modulation for electric power conversion", Proc.IEEE, vol.82, pp.1194-1214, Aug. 1994.
- [2] J. O. P. Pinto, B. K. Bose, L. E. B. Silva, M. P. Karmierkowski "A Neural Network Based Space Vector PWM Controller for Voltage-Fed Inverter Induction Motor Drive", IEEE Trans. on Ind. Appl., vol.36, no. 6, November/December 2000.
- [3] A. Bakhshai, J. Espinoza, G. Joos, H. Jin. "A combined ANN and DSP approach to the implementation of space vector modulation techniques", in conf. Rec.IEEE -IAS Annu. Meeting, 1996, pp.934-940.
- [4] F. Harashima et al., "Applications of neural networks to power converter control", in conf. Rec.IEEE -IAS Annu. Meeting, 1989, pp.1086-1091.
- [5] M. R. Buhl and R. D. Lorenz, "Design and implementation of neural networks for digital current regulation of inverter drives", in conf. Rec.IEEE -IAS Annu. Meeting, 1991, pp.415-423.
- [6] J. W. Song, K. C. Lee, K. B. Cho, J. S. Won, " An adaptive learning current controller for field - oriented controlled induction motor by neural network", in Proc. IEEE -IECON'91, 1991, pp.469-474.
- [7] M. P. Karmierskowski et al., " Neural network current control of VS-PWM inverters ", in Proc. IPE'95, 1995, pp.1415-1420.
- [8] N.V.Nho, M. J. Youn, "Two-mode overmodulation in two level VSI using principle control between limit trajectories", CD-ROM Proc. PEDS 2003, pp.1274-1279
- [9] J. Holtz, W. Lotzkat, M. Khambadkone, "On continuous control of PWM inverters in the overmodulation range including the six-step mode", IEEE Trans. Power Electron. , vol.8, pp.546-553, Oct. 1993.
- [10] S. Bolognani, M. Ziglitti, "Novel digital continuous control of SVM inverters in the overmodulation range", IEEE Trans. Ind. Applicat., vol.33, pp.525-530, Mars/ April 1997.